

# MAPPING NORTHERN AUSTRALIA'S PRESENT DAY STRESS FIELD: THE CANNING BASIN

**Adam Bailey\***  
Geoscience Australia  
Canberra, ACT  
adam.bailey@ga.gov.au

**Paul Henson**  
Geoscience Australia  
Canberra, ACT  
paul.henson@ga.gov.au

*\*presenting author*

## SUMMARY

The Canning Basin of Western Australia has recently become a site of interest for unconventional hydrocarbons, with several formations within deeper basin depocentres being investigated for resources. Modern petroleum resource evaluation is generally dependent on an understanding of both local and regional stresses, as well as the geomechanical properties of reservoir units. Presently, there are significant gaps in our understanding of these factors within the Canning Basin. This study is part of a greater effort from Geoscience Australia to understand the present-day stress field of northern Australia.

A generally NE-SW oriented maximum horizontal stress azimuth is identified from interpretation of borehole failure in five petroleum wells, and a broadly strike-slip faulting stress regime is interpreted from wireline data and wellbore testing. Variations in stress regime at different crustal levels within the Canning Basin are highlighted by one-dimensional mechanical earth models that show changes in the stress regime with depth as well as by lithology, with a general move towards a normal faulting stress regime at depths greater than ~2.5 km.

**Key words:** Canning Basin, present-day stresses, rock mechanics, image logs, unconventional petroleum

## INTRODUCTION

The Canning Basin (Figure 1) is one of Australia's most prospective onshore petroleum basins, with proven petroleum systems and current production from conventional reservoirs. There has also been recent interest in unconventional hydrocarbons within the deeper basin depocentres, particularly the Ordovician Goldwyer Formation and the Lower Carboniferous Laurel Formation. Knowledge of contemporary stresses can provide important information for understanding large-scale processes, such as intraplate deformation, as well as geodynamic and neotectonic processes. Regional and local stresses have implications for the mining, petroleum, and geothermal industries; understanding the stress regime and geomechanical properties of reservoir units are some of the critical factors required to determine a basin's resource potential. Fluid flow pathways within the sub-surface units are controlled by regional and local stresses and so understanding the present-day stress regime is integral to modern petroleum resource evaluation. Orientations and magnitudes of present-day stresses also have implications for borehole stability, water-flood design, and fault reactivation. This study characterises the regional stress regime at different crustal levels within the Canning Basin using existing well data and well tests to derive stress magnitudes and orientations, contributing to a greater effort from Geoscience Australia to understand the present-day stress field of northern Australia.

## METHOD AND RESULTS

This study was undertaken using publicly available data from Canning Basin petroleum wells accessed via the Western Australia Petroleum & Geothermal Information Management System (WAPIMS). Data from five petroleum wells (Table 1; Figure 1) were used to derive stress parameters from which a whole-of-basin representation of the present-day stress regime was constructed (Figure 2). The wells were selected due to their hosting electrical resistivity image logs, which are integral for understanding the orientation of the present-day stresses. Stress magnitudes were constrained using geophysical logs, wellbore tests, and rock properties to build both a general model of present-day basin stresses (Figure 2) and one-dimensional mechanical earth models (1D-MEMs) for each of the five wells (Figure 3).

Two main wellbore failures are commonly used as indicators of the maximum horizontal stress ( $\sigma_H$ ) azimuth: borehole breakouts (BO) and drilling induced tensile fractures (DITF). The removal of rock during the drilling process results in stress concentrations at the borehole wall; circumferential stress is maximised at the minimum horizontal stress azimuth and minimised at the maximum horizontal stress azimuth. This can lead to the wellbore spalling to form BOs in the minimum horizontal stress azimuth and the formation of large tensile fractures in the maximum horizontal stress azimuth. All five of the wells' interpreted image logs hosted populations of BOs, and only one well (Nicolay-1) hosted no observable DITF (Table 1). Thus, a reliable measurement of  $\sigma_H$  azimuth of  $56.7^\circ$  was derived from A-D quality indicators, as defined by the World Stress Map project (Heidbach et al., 2010). Application of the Rayleigh Test (Mardia, 1975) demonstrated that these data represent a non-random distribution.

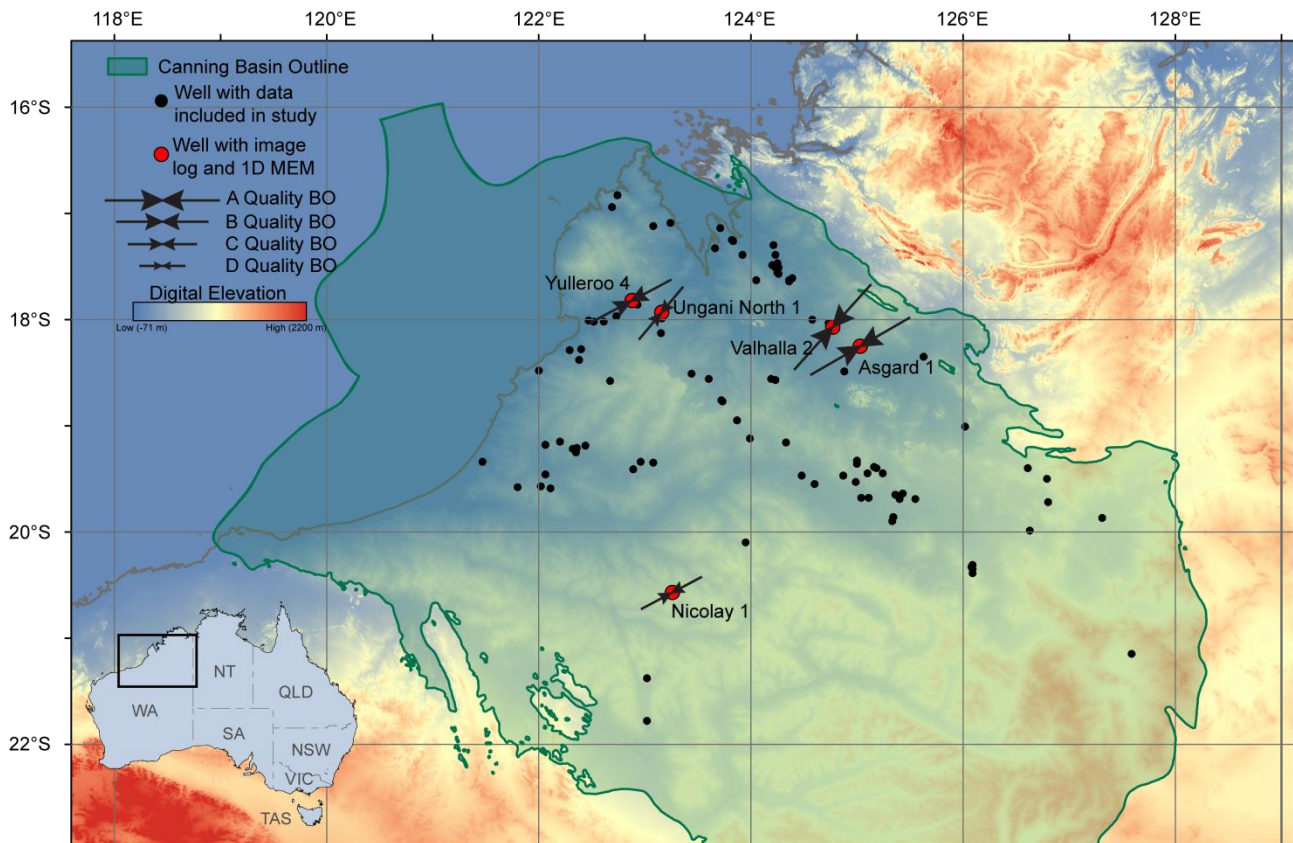


**Figure 1:** Map of the Canning Basin demonstrating maximum horizontal stress orientations from petroleum wells in this study. Quality of stress orientations is based on the criteria of the World Stress Map quality ranking system (Heidbach et al., 2010). Wells interpreted for stress indicators in this study are marked in red; all other wells which were investigated for further wireline or well testing data are marked in black. Digital elevation is SRTM-derived 3 second DEM data (Geoscience Australia, 2011).

The vertical, or overburden, stress ( $\sigma_v$ ) is controlled by the mass of overburden present over a given depth, and is generally calculated through an integration of bulk rock density (Bell, 1996). However, density logs are not always run to surface and so are often calibrated using the empirically derived Gardner (Gardner et al., 1974) velocity-density transform (Tingay et al., 2003) to estimate a top-of-log stress value from well velocity survey data (Zoback, 2007). This transform can be locally calibrated by laterally shifting the transform curve to pass through the average values on a cross plot of velocity ( $\text{km s}^{-1}$ ) and density ( $\text{g cm}^{-3}$ ) for a given well (after Tingay et al., 2003; King et al., 2010). Density logs from 102 open-file petroleum wells (Figure 1) were used to characterise  $\sigma_v$ , resulting in a mean  $\sigma_v$  magnitude of  $22.1 \text{ MPa km}^{-1}$  (standard deviation (s.d.) =  $1.0 \text{ MPa km}^{-1}$ ). Calculated magnitudes range from  $20.5 \text{ MPa km}^{-1}$  to  $25.0 \text{ MPa km}^{-1}$  at 1 km depth below the ground surface (Bailey et al., in prep.). Significant variations in  $\sigma_v$  magnitude are observed (Figure 2), and are primarily attributed to the presence of thick carbonate intervals in the Barbwire Terrace, the Devonian Reef Complexes of the northern Lennard Shelf, and the Mowla Terrace (Bailey et al., in Prep).

Well	Borehole Breakouts					Drilling Induced Tensile Fractures				
	Orientation (°)	Number	Length (m)	S.D.	Quality	Orientation (°)	Number	Length (m)	S.D.	Quality
Asgard 1	60.2	253	896.6	9.1	A	59.1	53	148.6	3.9	A
Nicolay 1	58.2	33	78.4	24.1	C					E
Ungani North 1	35.7	129	662.8	51.1	E	81.1	21	52.3	31.0	D
Valhalla 2	42.5	54	219.2	11.5	A	46.7	52	328.2	12.4	B
Yulleroo 4	62.1	116	526.6	13.6	B	65.1	5	13.1	1.9	D

**Table 1:** Maximum horizontal stress azimuth details for all interpreted wellbore image logs. Interpretation details are noted for both borehole breakout and drilling induced tensile fracture derived maximum horizontal stress orientation for each well. Quality rankings are according to the World Stress Map project guidelines (Heidbach et al., 2010)

Leak off tests (LOT) allow for direct determination of the minimum horizontal stress ( $\sigma_h$ ) magnitude (Bell, 1990). Results of 24 LOTs from 20 Canning basin wells were analysed in this study, using two different approaches to calculate  $\sigma_h$  magnitude. Several LOT results suggested unreasonably low  $\sigma_h$  magnitudes, and so these values were re-evaluated using the approach of Couzens-Schultz and Chan (2010) which assumes testing reactivates an existing fracture in shear rather than creating a new fracture under tension (e.g. Bailey et al., 2016). A mean value for  $\sigma_h$  magnitude of 18.5 MPa km<sup>-1</sup> is calculated from values that range from 3.2 MPa at 193 m depth to 58.2 MPa at 2644 m depth.

Numerous methods for estimating the magnitude of the maximum horizontal stress ( $\sigma_H$ ) exist; however, many of these are dependent on the presence of appropriate data quality. This study utilises the frictional limits method (Jaeger & Cook, 1979) in order to provide an upper limit to possible  $\sigma_H$  values, as well as attempting to directly estimate  $\sigma_H$  from known relationships between circumferential stress and the presence of DITFs in a given vertical well (Brudy & Zoback, 1999). Application of the frictional limits method results in values that range from 26.3 MPa km<sup>-1</sup> to 45.8 MPa km<sup>-1</sup>, for a mean  $\sigma_H$  gradient of 35.9 MPa km<sup>-1</sup>. Circumferential stress estimates are made using the following equation (Brudy & Zoback, 1999):

$$\sigma_H = 3(\sigma_h) - P_w - P_p - T \tag{Equation (1)}$$

Where  $P_w$  is wellbore pressure (calculated from mud weight),  $P_p$  is pore pressure (assumed to be hydrostatic), and  $T$  is tensile rock strength (assumed to be 0 when DITFs are observed). Calculated values of  $\sigma_H$  from equation (1) vary from 4.3 MPa at 193 m depth to 87.8 MPa at 2644 m depth, for a mean  $\sigma_H$  gradient of 26.9 MPa km<sup>-1</sup>.

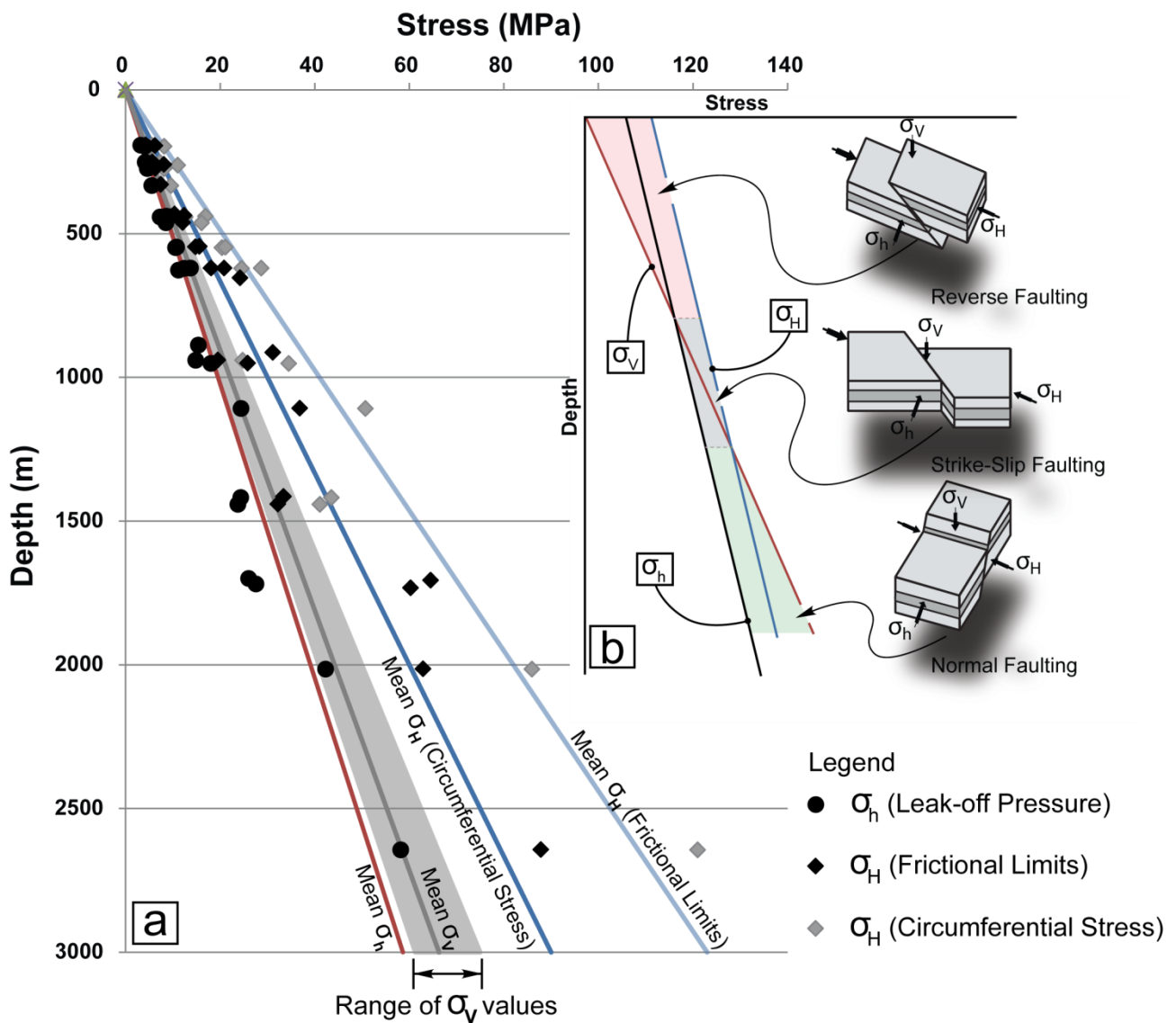


Figure 2: (A) Depth (m) vs stress (MPa) illustrating the magnitudes of the three principal stresses in the Canning Basin, as calculated from well test leak-off pressures (minimum horizontal stress), density integrations (vertical stress) and the circumferential stress and frictional limits methods (maximum horizontal stress). Broadly, these data define a strike-slip faulting stress regime for the Canning Basin, and; (B) inset showing the relationship between principal stress relative magnitudes and faulting regime (after Brooke-Barnett et al., 2015)

Detailed 1D MEMs can be constructed using poroelastic stress equations (Thiercelin and Plumb, 1994) that take tectonic strain into consideration (e.g. Brooke Barnett et al., 2015):

$$\sigma_H = \frac{V_{stat}}{1-V_{stat}}(\sigma_V - \alpha P_p) + \alpha P_p + \frac{E_{stat}}{1-V_{stat}^2}(\epsilon_{max} + V_{stat}\epsilon_{min}) \quad \text{Equation (2)}$$

$$\sigma_h = \frac{V_{stat}}{1-V_{stat}}(\sigma_V - \alpha P_p) + \alpha P_p + \frac{E_{stat}}{1-V_{stat}^2}(\epsilon_{min} + V_{stat}\epsilon_{max}) \quad \text{Equation (3)}$$

Where  $V_{stat}$  is the statically corrected Poisson's ratio (unitless),  $\alpha$  is the Biot's poroelastic coefficient (unitless, assumed  $\alpha=1$ ),  $E_{stat}$  is the statically corrected Young's modulus (Pa),  $\epsilon_{min}$  is strain in the minimum stress direction (unitless), and  $\epsilon_{max}$  is the strain in the maximum stress direction (unitless). Dynamic Poisson's ratio and Young's modulus were derived from logged compressional and shear sonic data in each well, and calibrated to static laboratory measurements obtained through previous triaxial testing in Canning Basin wells (Wu et al., 2000; Terratek, 2013; Delle Piane et al., 2015). Empirical relationships were used to derive compressive rock strength values (Chang et al., 2006). Numerous reliable hydraulic fracture tests at multiple depths are required in order to appropriately calibrate 1D MEMs. Calibration can also be achieved through modelling of observed BO in image logs, where those BOs have been imaged in sufficient quality to accurately assess opening angle (Moos and Zoback, 1990). Five 1D MEMs were constructed in this study, however, accurate calibration is challenging due to the majority of available LOTs having been conducted at depths of <1 km. Each test is calibrated on suitable LOTs using an iterative process of adjusting strain values from initial values of 0.0009 for strain in the maximum stress direction and 0.0003 for strain in the minimum stress direction. In order to draw more than broad inferences from these data, detailed borehole failure modelling must be undertaken to more precisely calibrate the 1D MEMs.

Calibrated stress profiles within the Canning Basin demonstrate a dominantly strike-slip faulting stress regime, with a gradual shift towards a normal faulting stress regime at depths greater than ~2.5 km (Figure 3). Shallow regions of the basin are not well covered in these data, however, 1D MEMs from Asgard 1, Ungani North 1, and Yulleroo 4 all feature data from depths shallower than 1 km that suggests the presence of a reverse- to strike-slip faulting stress regime near the basin surface (Figure 3). A strike-slip faulting stress regime is observed from ~1 km to ~2.5 km depth (Figure 3). Transitional zones, where two or more principal stresses are close to each other in magnitude (or where there is variation in which stress is the maximum, intermediate, or minimum), exist throughout the section and are mostly due to lithological variations. A strong association between lithology and present-day stress magnitudes is observed; thick sandstone and carbonate intervals exhibit elevated  $\sigma_H$  magnitudes that in some instances result in lithology restricted changes to the stress regime, particularly at depths greater than 2.5 km where raised  $\sigma_H$  magnitudes result in a shift from a normal faulting stress regime back to a strike slip faulting stress regime, or to transitional stress regimes (Figure 3). Previous earthquake focal mechanisms data suggests a likely reverse-faulting stress regime from several events located in the NW corner of the Kidson Sub-Basin (Denham et al., 1974; Fredrich et al., 1988), however, these events are thought to originate from a depth of approximately 8 ( $\pm 3$ ) km. While this is in the upper section of the crust, the maximum thickness of the Kidson Sub-Basin is thought to be ~5 km (Department of Mines and Petroleum, 2017), and so these events likely occurred within the underlying basement and not the sedimentary succession which is the subject of this study (Fredrich et al., 1988).

## CONCLUSIONS

Wireline data interpretation reveals a variable present-day state of stress in the Canning Basin of Western Australia. An approximately NE-SW orientation is interpreted from observed wellbore failure in five wells' electrical resistivity based image logs. This orientation is in agreement with earthquake focal mechanisms from the region (e.g. Denham et al., 1974). Broadly, interpreted data from wireline logs and wellbore testing implies that  $\sigma_h < \sigma_v < \sigma_H$ , describing a strike-slip faulting stress regime for the Canning Basin. However, 1D MEMs constructed for five wells highlight the relationship between lithology and stress. Lithological effects result in variation to the overall strike-slip faulting stress regime, with transitional stress regimes being likely (e.g. strike-slip to normal faulting). Additionally, there is a general trend evident, from a transitional reverse- to strike-slip faulting stress regime in the top ~1 km of the basin, through a strike-slip faulting stress regime to ~2.5 km depth, with lithology driven transitional strike-slip to normal faulting conditions becoming prevalent at depths greater than ~2.5 km. Due to a less than desirable quantity of calibrating data, these 1D MEMs should be treated with care. Further, localised, variation of the present-day stress regime is likely, due to large  $\sigma_v$  magnitude variations across the basin. Further development of this work requires the acquisition of further rock testing data for tighter 1D-MEM calibration. Rock property information for each formation intersected would allow for localised calibrations (rather than relying on basin-wide relationships); further, borehole failure modelling should also be attempted.

## ACKNOWLEDGMENTS

The authors would like to acknowledge the Western Australian Department of Mines, Industry Regulation, and Safety for their assistance in locating and providing well data. Particular thanks are reserved for Eric Tenthorey and Chris Southby at Geoscience Australia for their input in improving this study, and for Mojtaba Rojabi at the University of Adelaide for his ongoing work providing up-to-date stress data for the Australian Continent. This paper is published with the permission of the CEO of Geoscience Australia.

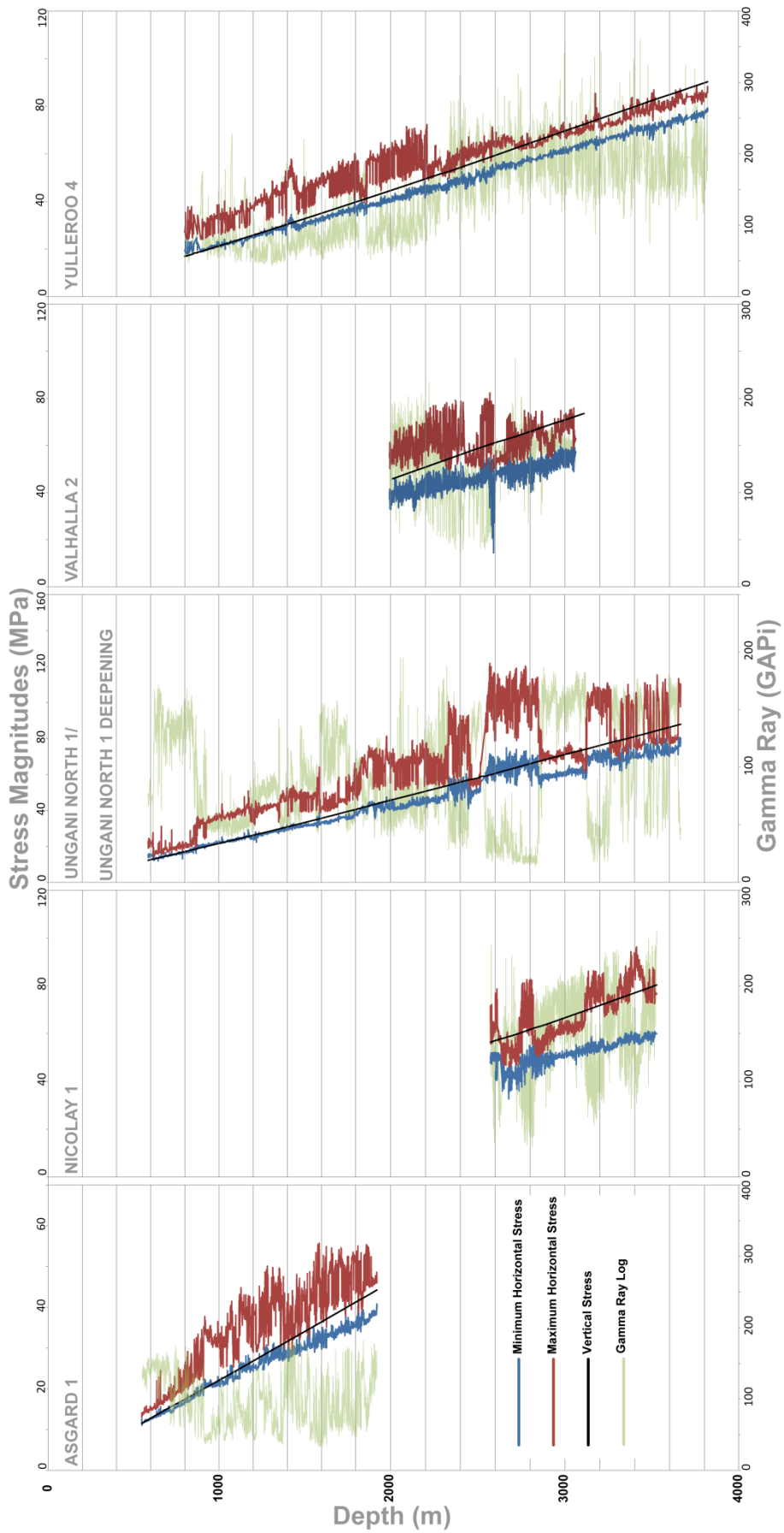


Figure 3: One-dimensional mechanical earth models constructed for the five wells identified in Table 1.

## REFERENCES

- Bailey, A. H., King, R. C., Holford, S. P., and Hand, M., 2016, Incompatible stress regimes from geological and geomechanical datasets: Can they be reconciled? An example from the Carnarvon Basin, Western Australia: *Tectonophysics*, 683, 405–416.
- Bailey, A., In Prep, Variations of vertical stress in the Canning Basin, Australia (working title).
- Bell, J. S., 1990, Investigating stress regimes in sedimentary basins using information from oil industry wireline logs and drilling records: In Hurst, A., and Lovell, M. A. (Eds.), *Geological applications of wireline logs* (Vol. 48, pp. 305–325). London, UK: Geological Society of London, Special Publication.
- Bell, J. S., 1996, *Petro Geoscience*. 1. In situ stresses in sedimentary rocks. 1. Measurement techniques: *Geoscience Canada*, 23(2), 85–100.
- Brooke-Barnett, S., Flottmann, T., Paul, P., Buseti, S., Hennings, P., Reid, R., and Rosenbaum, G., 2015, Influence of basement structures on in situ stresses over the Surat Basin, southeast Queensland: *Journal of Geophysical Research: Solid Earth*, 120(7), 4946–4965.
- Brudy, M., and Zoback, M. D., 1999, Drilling-induced tensile wall-fractures: Implications for determination of in-situ stress orientation and magnitude: *International Journal of Rock Mechanics and Mining Sciences*, 36, 191–215.
- Chang, C., Zoback, M. D., and Khaksar A., 2006, Empirical relations between rock strength and physical properties in sedimentary rocks, *Journal of Petroleum Science and Engineering*: 51, 223–237.
- Couzens-Schultz, B. A., and Chan, A. W., 2010, Stress determination in active thrust belts: An alternative leak-off pressure interpretation: *Journal of Structural Geology*, 32, 1061–1069
- Department of Mines and Petroleum, 2017, Summary of Petroleum Prospectivity: Canning Basin, February 2017. Petroleum Division, Department of Mines and Petroleum, Perth, 22 pp.
- Delle Piane, C., Almqvist, B. S., MacRae, C. M., Torpy, A., Mory, A. J., and Dewhurst, D. N., 2015, Texture and diagenesis of Ordovician shale from the Canning Basin, Western Australia: Implications for elastic anisotropy and geomechanical properties. *Marine and Petroleum Geology*, 59, 56–71.
- Denham, D., Everingham, I. B., and Gregson, P. J., 1974, East Canning basin earthquake, March 1970: *Journal of the Geological Society of Australia*, 21(3), 353–358.
- Fredrich, J., McCaffrey, R., and Denham, D., 1988, Source parameters of seven large Australian earthquakes determined by body waveform inversion: *Geophysical Journal International*, 95(1), 1–13.
- Gardner, G. H. F., Gardner, L. W., and Gregory, A. R., 1974, Formation velocity and density—the diagnostic basics for stratigraphic traps: *Geophysics*, 39, 770–780.
- Geoscience Australia, 2011, SRTM-derived 3 Second Digital Elevation Models Version 1.0: Record 72760 (<http://www.ga.gov.au/metadata-gateway/metadata/record/72760/>): Last accessed 24<sup>th</sup> August 2017.
- Heidbach, O., Tingay, M., Barth, A., Reinecker, J., Kurfess, D., and Mueller, B., 2010, Global crustal stress pattern based on the World Stress Map database release 2008: *Tectonophysics*, 482(1–4), 3–15.
- Jaeger, J. C., and Cook, N. G. W., 1979, *Fundamentals of rock mechanics* (3rd ed.). London, UK: Chapman & Hall.
- King, R. C., Neubauer, M., Hillis, R. R., and Reynolds, S. D., 2010, Variation of vertical stress in the Carnarvon Basin, NW Shelf, Australia: *Tectonophysics*, 482, 73–81.
- Mardia, K. V., 1975, Statistics of Directional Data, *Journal of the Royal Statistical Society, Series B* (Methodological), 37(3), 349–393
- Moos, D., and M. D. Zoback, 1990, Utilization of observations of well bore failure to constrain the orientation and magnitude of crustal stresses: Application to continental deep sea drilling project and ocean drilling program boreholes: *Journal of Geophysical Research*, 95, 9305–9325
- Terratek, 2013, Integrated tight rock analysis: Rotary sidewall cores – Valhalla North 1 Well, Western Australia: Terratek report TR12-810865 (Prepared for Buru Energy)
- Thiercelin, M., and R. Plumb, 1994, Core-based prediction of lithologic stress contrasts in east Texas formations: *SPE Formation Evaluation*, 9(4), 251–258.
- Tingay, M. R. P., Hillis, R. R., Morley, C. K., Swarbrick, R. E., and Okpere, E. C., 2003, Variation in vertical stress in the Baram Basin, Brunei: Tectonic and geomechanical implications: *Marine and Petroleum Geology*, 20, 1201–1212.
- Wu, B., Tan, C.P., and Connelly, L., 2000, Elastic and strength properties of Yulleroo-1 Sandstone: CSIRO Petroleum Report No. 00-035
- Zoback, M. D., 2007, *Reservoir geomechanics*. New York, NY: Cambridge University Press